1521-009X/46/5/697–703$35.00
DRUG METABOLISM AND DISPOSITION

https://doi.org/10.1124/dmd.117.079467
Drug Metab Dispos 46:697–703, May 2018

Special Section on Transporters in Drug Disposition and Pharmacokinetic Prediction

MRP2 Inhibition by HIV Protease Inhibitors in Rat and Human Hepatocytes: A Quantitative Confocal Microscopy Study[S]

Nico Holmstock, Marlies Oorts, Jan Snoeys, and Pieter Annaert

Drug Delivery and Disposition, KU Leuven Department of Pharmaceutical and Pharmacological Sciences, O&N2, Leuven, Belgium (N.H., M.O., P.A.) and Janssen Research and Development, Beerse, Belgium (J.S.)

Received November 11, 2017; accepted March 7, 2018

ABSTRACT

Hepatic drug transporters play a pivotal role in the excretion of drugs from the body, in drug-drug interactions, as well as in drug-induced liver toxicity. Hepatocytes cultured in sandwich configuration are an advantageous model to investigate the interactions of drug candidates with apical efflux transporters in a biorelevant manner. However, the commonly used "offline" assays (i.e., that rely on measuring intracellular accumulated amounts after cell lysis) are time- and resource-consuming, and the data output is often highly variable. In the present study, we used confocal microscopy to investigate the inhibitory effect of all marketed HIV protease inhibitors (10 μM) on the apical efflux transporter multidrug resistance–associated protein 2 (MRP2; ABCC2) by visualizing the biliary accumulation of the fluorescent substrate 5(6)-carboxy-2′,7′-dichlorofluorescein (CDF). This method was applied with sandwich-cultured human and rat hepatocytes. Alterations in the biliary excretion index of CDF were calculated on the basis of quantitative analysis of fluorescence intensities in the confocal images. In human hepatocytes, lopinavir followed by tipranavir, saquinavir, atazanavir, and darunavir were the most potent inhibitors of MRP2-mediated efflux of CDF. In rat hepatocytes, tipranavir inhibited Mrp2-mediated CDF efflux most potently, followed by lopinavir and nelfinavir. In conclusion, a comparison of these findings with previously published data generated in offline transporter inhibition assays indicates that this microscopy-based approach enables investigation of the inhibitory effect of drugs on efflux transporters in a very sensitive but nondestructive manner.

Introduction

Drug-induced hepatotoxicity and adverse drug reactions are commonly encountered phenomena during the drug development process. Interactions of drugs with hepatic drug transporters have been implicated in some of these adverse effects (Giacomini et al., 2010). Hepatic drug transporters play an important role in the disposition of many drugs but also of several endogenous compounds, such as bilirubin and bile acids. It follows that these transporters are important sites of interaction, since competition for the same transporter binding sites may emerge between multiple coadministered drugs on the one hand, and between drugs and endogenous compounds on the other. This competition often leads to alterations in the pharmacokinetics and/or toxicity of drugs but can also pose problems regarding the homeostasis of endogenous compounds (e.g., in case of cholestasis). This implies that during drug development it is very important to determine the possible modulatory effects of drug candidates toward drug transporters.

Several model systems are available to explore the transport kinetics of drug candidates by drug transporters. Interaction with uptake transporters is frequently studied using transfected cell lines expressing one specific transporter (Annaert et al., 2010) or using hepatocytes (suspension of in culture) (De Bruyn et al., 2013). Freshly isolated or cryopreserved hepatocytes have the advantage of concomitantly expressing the main uptake transporters (for some of them at levels comparable to the in vivo situation), which allows insight into the contribution of each transporter to drug uptake (Badée et al., 2015). Considering efflux transporters, available model systems include inside-out membrane vesicles, either prepared from liver tissue (Guyot et al., 2014) or from cells expressing one specific transporter (Köck and Brouwer, 2012), as well as suspended or sandwich-cultured hepatocytes (SCH) (De Bruyn et al., 2013). More specifically, the expression levels of the basolateral efflux transporters MRP3 (*ABCC3*) and MRP4 (*ABCC4*) have been shown to be comparable between suspended hepatocytes and the in vivo situation, and some apical (canalicular) efflux transporters were shown to undergo partial internalization (Bow et al., 2008; Lundquist et al., 2014). Importantly, culturing hepatocytes in sandwich configuration for multiple days allows the formation of bile canaliculi and the proper localization of the apical transporters, which makes it a preferred in vitro model to study expression, function, and regulation of the apical efflux transporters (De Bruyn et al., 2013).

This research was funded by a research and development (O&O) grant from the Institute for the Promotion of Innovation through Science and Technology in Flanders (IWT). The Nikon A1R Eclipse Ti confocal microscope was acquired through a Hercules type 1 AKUL/09/037 grant to Wim Annaert.

https://doi.org/10.1124/dmd.117.079467.

[S]This article has supplemental material available at dmd.aspetjournals.org.

ABBREVIATIONS: BEI, biliary excretion index; CDF, 5(6)-carboxy-2′,7′-dichlorofluorescein; CDFDA, CDF diacetate; Mrp2/MRP2, multidrug resistance-associated protein 2; SCH, sandwich-cultured hepatocytes; SCHH, sandwich-cultured human hepatocytes; SCRH, sandwich-cultured rat hepatocytes; WEM, William's E medium.

The present study introduces a nondestructive technique whose basis is confocal microscopy to quantitatively measure the Mrp2/MRP2 inhibition in rat and human hepatocytes in sandwich culture using CDF, a well characterized fluorescent substrate of MRP2/Mrp2 (Bow et al., 2008; Heredi-Szabo et al., 2008; Ye et al., 2010; Wissel et al., 2015). The inhibitory effect of all marketed HIV protease inhibitors on the Mrp2/MRP2 activity was quantified by determining changes in the biliary excretion index (BEI) of CDF in the presence of these antiretroviral drugs. Antiretroviral drugs currently used in the treatment of HIV infection were chosen as the model drugs. They often play an important role in many profound drug-drug interactions in the clinic. Moreover, their hepatic disposition constitutes a complex interplay between uptake, metabolism, and efflux. These drugs are taken up by the Oatp/OATP family, metabolized by CYP3A enzymes, and excreted by the efflux transporters Mdr1/MDR1 and Mrp2/MRP2 (Huisman et al., 2002; Liu and Unadkat, 2013; De Bruyn et al., 2016).

Finally, the results obtained from the present study were compared with previously published data resulting from a conventional ("offline") approach in sandwich-cultured rat and human hepatocytes (SCRH and SCHH) (Ye et al., 2010).

Materials and Methods

Chemicals

Darunavir ethanolate, tipranavir, ritonavir, atazanavir sulfate, and amprenavir were provided by the National Institutes of Health AIDS Research and Reference Reagent Program (Germantown, MD). Saquinavir mesylate, indinavir sulfate, nelfinavir mesylate, and lopinavir were donated by Hetero Drugs Ltd. (Hyderabad, India). William's E medium (WEM), Dulbecco's modified Eagle's medium (DMEM), L-glutamine, penicillin-streptomycin (each 10,000 IU/ml), fetal bovine serum, Hanks' balanced salt solution (HBSS), and phosphate buffered saline (PBS) were purchased from Westburg (Leusden, The Netherlands). ITS$^+$ universal culture supplement premix was from BD Biosciences (Erembodegem, Belgium). HEPES was purchased from MP Biochemical (Illkirch, France). Collagenase (Type IV), dexamethasone, insulin from human origin, 5(6)-Carboxy-2′,7′-dichlorofluorescein diacetate (CDFDA), Percoll, and ECM gel (from Engelbreth-Holm-Swarm murine sarcoma) were purchased from Sigma-Aldrich (Schnelldorf, Germany). Synth-a-Freeze was purchased from Life Technologies Europe (Ghent, Belgium).

Methods

Animals. Male Wistar rats in a weight range of 170–200 g were purchased from Janvier (Le Genest Saint Isle, France) and were used for isolation of hepatocytes. The animals were housed in the Central Animal Facilities of KU Leuven, according to the Belgian and European laws, guidelines, and policies for animal experimentation, housing, and care. Approval for the experiments was granted by the Institutional Ethical Committee for Animal Experimentation of the KU Leuven. Rats were maintained in a 12-hour light-dark cycle with free access to water and standard rat/mouse maintenance food (ssniff Spezialdiäten GmbH, Soest, Germany).

Isolation and Cryopreservation of Rat Hepatocytes. Rat hepatocytes were isolated using a two-step collagenase perfusion, as previously described (Annaert et al., 2001). Rats were anesthetized using an intraperitoneal injection (120 mg/kg ketamine + 24 mg/kg xylazine i.p.). After isolation, cells were centrifuged (50*g*) for 3 minutes at 4°C and the pellet was resuspended in WEM containing 5% FBS, 2 mM L-glutamine, 100 IU/ml penicillin, and 100 μg/ml streptomycin. The hepatocytes were counted three times in a hemocytometer, and the viability was determined using the Trypan blue (0.04%) exclusion method. After counting, the hepatocytes were either cultured freshly or cryopreserved for later use. For cryopreservation, cells were again centrifuged at 50*g* for 3 minutes at 4°C and the pellet was resuspended in Synth-a-Freeze at a cell density of 10×10^6 cells/ml. Cells were cryopreserved in a programmable controlled-rate freezer, Kryo 560–16 (Planer, Sunbury-on-Thames, UK), during a freezing cycle that included a supercooling phase. After reaching −100°C, the cryovials were stored in liquid nitrogen until thawing.

Sandwich-Cultured Rat Hepatocytes. Cryopreserved rat hepatocytes were quickly thawed in a 37°C water bath. When all ice was melted, the content was transferred to a mixture of isotonic Percoll (32%) and thawing medium (DMEM supplemented with 10% FBS, 2 mM L-glutamine, 100 IU/ml penicillin, 100 μg/ml streptomycin, 4 μg/ml insulin, and 1 μM dexamethasone) (68%). The cells were centrifuged at 168*g* for 20 minutes at 22°C. Subsequently, the pellet was resuspended in thawing medium and centrifuged at 50*g* for 3 minutes at 22°C. Next, the cells were resuspended in seeding medium (WEM containing 10% FBS, 2 mM L-glutamine, 100 IU/ml penicillin, 100 μg/ml streptomycin, 4 μg/ml insulin, and 1 μM dexamethasone) at a density of 1.2 million cells/ml. The hepatocytes were then seeded in glass-bottom 24-well plates at a density of 26×10^4 cells/cm^2 and placed in an incubator (37°C, 5% CO_2, 95% humidity) (BINDER CO_2 incubator; Tuttlingen, Germany). These 24-well plates with glass bottoms and a thickness of 160–190 μm (MatTek, Ashland, MA) were precoated 24 hours before seeding with 50 μg/ml collagen diluted in 0.02 M acetic acid ("rigid collagen"). The wells were washed three times with PBS before seeding. Unattached cells were aspirated 2 hours after seeding by shaking the plate and immediately aspirating the media. Subsequently, cultures were overlaid with ice-cold neutralized collagen solution (~1.5 mg/ml, pH 7.4) to obtain a sandwich configuration. After 40 minutes, seeding medium was added to the SCH. The medium was replaced every 24 hours with maintenance medium (WEM supplemented with 1% ITS$^+$ universal culture supplement premix, 2 mM L-glutamine, 100 IU/ml penicillin, 100 μg/ml streptomycin, and 0.1 μM dexamethasone). Cells were used at day 3 of culture time.

Sandwich-Cultured Human Hepatocytes. Human cryopreserved hepatocytes for sandwich culture (batch no. S2203LT) were kindly provided by KaLy-Cell (Plobsheim, France) and were from a Caucasian, 59-year-old woman who had died from a colorectal adenocarcinoma. The hepatocytes were quickly thawed in a 37°C water bath. When all ice was melted, the content was transferred to a mixture of isotonic Percoll (32%) and thawing medium (68%). The cells were centrifuged at 168*g* for 20 minutes at 22°C. Subsequently, the pellet was resuspended in thawing medium and centrifuged at 100*g* for 3 minutes at 22°C. Next, the cells were resuspended in seeding medium at a density of 1.2 million cells/ml. Viability of the thawed hepatocytes was 91%. The hepatocytes were then seeded in glass-bottom 24-well plates, precoated with rigid collagen (see above) at a density of 26×10^4 cells/cm^2 and placed in an incubator (37°C, 5% CO_2, 95% humidity). Next, the cells were overlaid with 0.25 mg/ml ECM gel in growing medium after 24 hours (day 1). The medium was replaced every 24 hours with fresh maintenance medium. Cells were used at culture day 6.

Imaging of CDF Efflux. The biliary excretory function of SCRH/SCHH was assessed by quantitative evaluation of the CDF efflux in biliary canalicular network. Cells were washed twice with standard buffer (HBSS buffered with 10 mM HEPES at pH 7.4), and then preincubated with standard buffer containing an HIV protease inhibitor (10 μM) for 10 minutes. Next, the cells were incubated with CDFDA (1 or 4 μM, as specified in the figure legends) for 10 minutes in the absence or presence of an HIV protease inhibitor (10 μM). All experiments were conducted at 37°C. The culture plate was then placed under a Nikon Eclipse Ti A1R Confocal microscope with a temperature control unit set at 37°C. Images were acquired using the FITC laser line with excitation wavelength 488 nm. The HV (gain) was set at 100 (default); offset-background was left at 0; laser power was set at 5%; the pinhole was set at 1.2 airy unit (AU). During picture acquisition, pixel intensity and saturation were monitored and, if required, laser power and HV were optimized to obtain adequate pixel intensities. For each condition, three images were taken of random locations within the well at a resolution of 1024 × 1024 pixels.

Calculation of BEI of CDF. ImageJ software (National Institutes of Health) was used for quantitative analysis of the fluorescent microscopic images. The average pixel intensity of the areas representing the bile canaliculi and cells was determined after manual selection of these regions on the basis of phase contrast images, taking into account background. The BEI was calculated according to the following formula:

$$BEI(\%) = \frac{\left(\sum pixel\ intensity\right)_{bile}}{\left(\sum pixel\ intensity\right)_{cells+bile}} \times 100 \quad (1)$$

Statistics. Statistical analysis was performed using one-way analysis of variance followed by Dunnett's test. P values less than 0.05 were considered statistically significant.

The Spearman rank correlation coefficient was determined between the obtained data in this study and previously published data obtained with the "offline" assay (Ye et al., 2010). This was done according to the following formula:

$$\rho = 1 - \frac{6\sum d_i^2}{n(n^2-1)} \quad (2)$$

where ρ is the Spearman rank correlation coefficient, d_i is the difference in ranks and n is the sample size.

Results

The BEI of CDF as a Function of Incubation Time. In a first phase of experiments, we investigated the optimal incubation time of SCRH with CDFDA to determine the BEI for CDF. This was done by using CDFDA (4 μM) in absence or presence of the well known MRP inhibitor MK-571 (10 and 30 μM). Time-lapse imaging showed that the BEI for CDF was constant during 10 minutes of incubation for all three conditions; the BEI was about 47% in the control condition, and MK-571 reduced it toward 10% at both tested concentrations (Fig. 1). Interestingly, although MK-571 at 30 μM clearly reduced the total fluorescence intensity in the image compared with MK-571 at 10 μM, both concentrations resulted in a similar BEI of CDF. As there was no influence of incubation time on BEI of CDF, we selected 10 minutes as incubation time for the next experiments.

The Effect of HIV Protease Inhibitors on the BEI of CDF in SCRH. The effect of all HIV protease inhibitors on the BEI of CDF in SCRH at culture day 3 was investigated. Figure 2 shows the images taken after 10 minutes of incubation with CDFDA (1 μM) in absence and presence of all HIV protease inhibitors (10 μM). These data clearly show a wide range in the inhibitory effect of HIV protease inhibitors on Mrp2-mediated CDF transport. Tipranavir had the most pronounced effect on the BEI of CDF, almost completely blocking the efflux of CDF into the bile canaliculi. This was followed by lopinavir, nelfinavir and saquinavir. Indinavir, atazanavir, ritonavir, and darunavir did not cause a statistically significant decrease in BEI of CDF. Amprenavir on the other hand increased the BEI of CDF by 24%.

The Effect of HIV Protease Inhibitors on the BEI of CDF in SCHH. The effect of all HIV protease inhibitors on the BEI of CDF was investigated in SCHH at culture day 6. Figure 3 shows the images taken after 10 minutes of incubation with CDFDA (1 μM) in absence and presence of all HIV protease inhibitors (10 μM). These data clearly show a wide range in the inhibitory effect of HIV protease inhibitors on MRP2. Lopinavir had the most pronounced effect on the BEI of CDF, almost completely blocking the efflux of CDF into the bile canaliculi. This was followed by tipranavir, saquinavir, atazanavir, and darunavir, respectively. Ritonavir, amprenavir, nelfinavir, and indinavir did not cause a statistically significant change in BEI of CDF.

Comparison between the Transporter Inhibition Data Presented Here and Data Previously Obtained from Conventional (Offline) Assay. The Spearman rank correlation coefficient was determined between the data obtained in this study using confocal microscopy and previously published data whose experimental basis was cellular accumulation and efflux (Ye et al., 2010). As tipranavir was not included in the study performed by Ye et al., this compound was not taken into account in the analysis. The ρ values obtained were 0.71 and 0.62 for the data from rat and human hepatocytes, respectively (Supplemental Table 1).

Discussion

The current study aimed to investigate the use of confocal microscopy to quantitate the inhibitory effect of all clinically relevant HIV protease inhibitors on the activity of Mrp2/MRP2 in SCRH and SCHH. SCH were used as the preferred in vitro model since hepatocytes cultured in a sandwich configuration have the ability to form functional biliary networks, and subsequently to maintain the presence of canalicular efflux transporters (LeCluyse et al., 1994; Lecluyse et al., 2000; De Bruyn et al., 2013). Over the past years, SCH have become the gold standard for hepatic in vitro studies, which allow exploration of the hepatic disposition of compounds, including uptake, metabolism, and efflux.

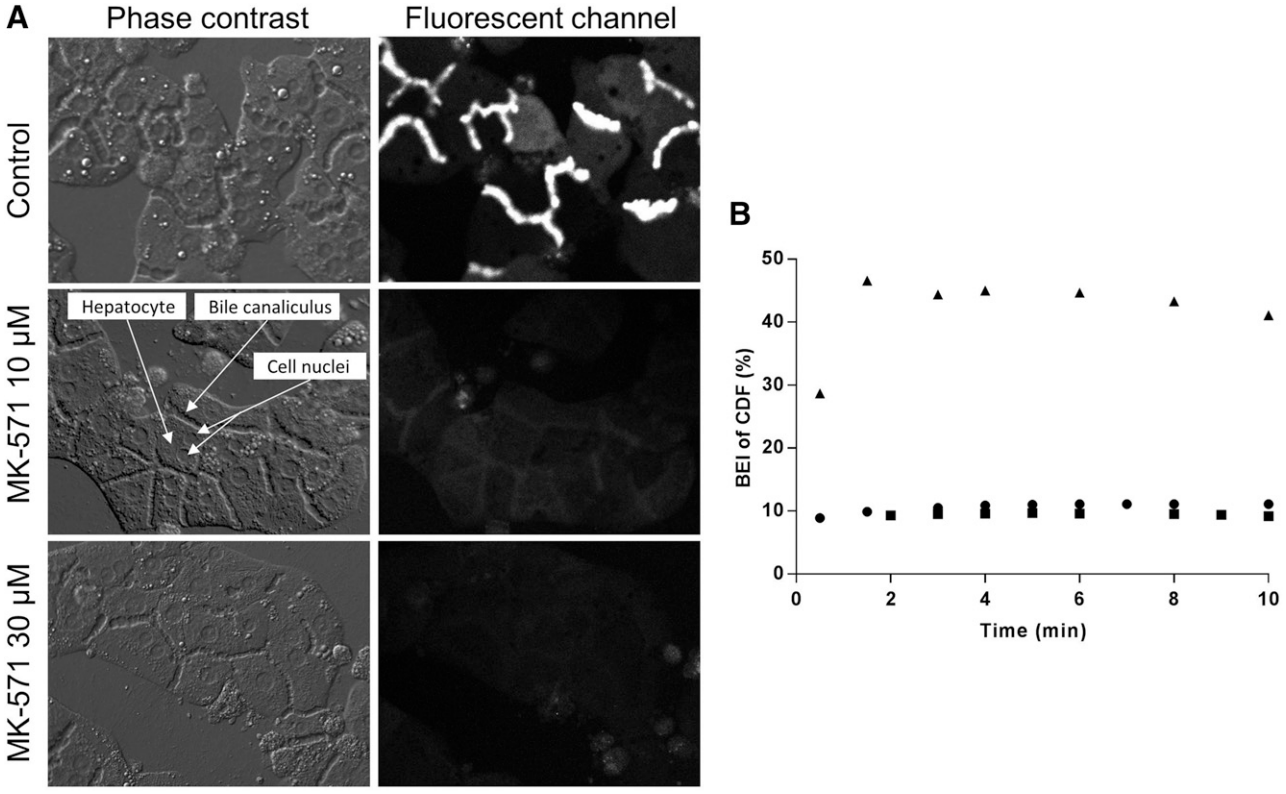

Fig. 1. The effect of MK-571 on the BEI of CDF in sandwich-cultured rat hepatocytes at culture day 3. (A) Phase contrast and fluorescence images of CDF accumulation in absence (control) and presence of MK-571 (10 and 30 μM). Images taken after 10 minutes of incubation with CDFDA (4 μM). (B) BEI of CDF as a function of incubation time in absence (▲) and presence of MK-571 at 10 (●) and 30 μM (■).

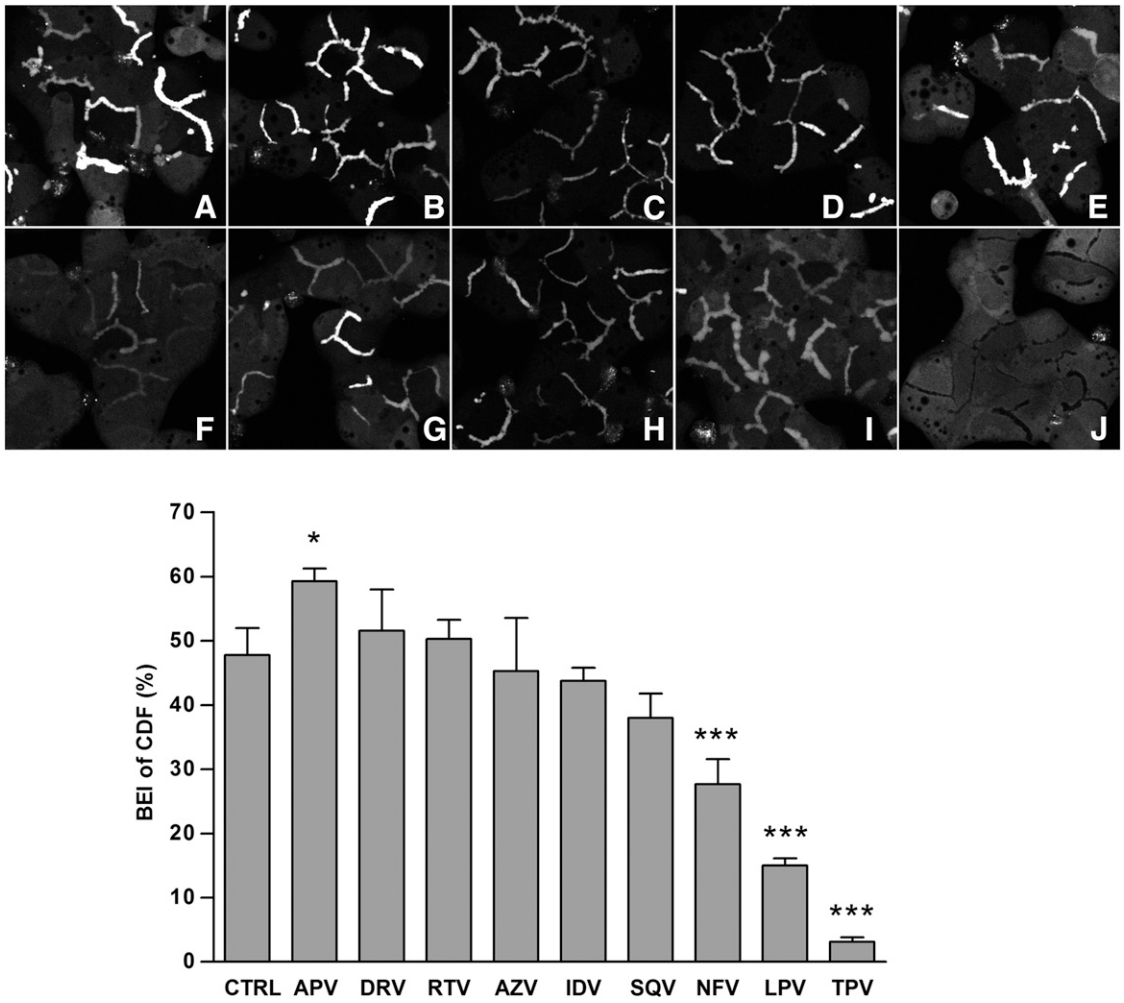

Fig. 2. Effect of HIV protease inhibitors on BEI of CDF in sandwich-cultured rat hepatocytes at culture day 3. Cells were preincubated with HIV protease inhibitors (10 μM) for 10 minutes, prior to incubation with CDFDA (1 μM) for 10 minutes in absence or presence of HIV protease inhibitors. (A) Control, (B) amprenavir (APV), (C) atazanavir (AZV), (D) darunavir (DRV), (E) indinavir (IDV), (F) lopinavir (LPV), (G) nelfinavir (NFV), (H) ritonavir (RTV), (I) saquinavir (SQV), and (J) tipranavir (TPV). Bars represent the mean ± S.D. (n = 3). Statistical significance between the different conditions was evaluated using one-way analysis of variance followed by Dunnett's test. Significantly different from control condition; $^{*}P < 0.05$; $^{***}P < 0.001$.

Using CDFDA in cell-based assays has the great advantage that it is nonfluorescent and passively diffuses inside cells, where it is rapidly hydrolyzed to fluorescent CDF. In rat hepatocytes, CDF was shown to be transported via Mrp2 into the bile and via Mrp3 into the sinusoidal blood, after which it can undergo cellular reuptake via Oatp-mediated transport (Zamek-Gliszczynski et al., 2003). Mrp2 was shown to carry out the majority of CDF efflux, but the role of Mrp3 was shown to increase in the absence of functional Mrp2 (Ellis et al., 2014). Confocal microscopy was used to visualize and quantify the fluorescence intensity inside the cells and the bile in all conditions tested. In that way, the BEI of CDF (reflecting the ratio of CDF in the bile canaliculi versus CDF in the cells plus bile canaliculi) could be determined. Eventually, this allowed investigation of the effects of HIV protease inhibitors on Mrp2/MRP2-mediated transport in a nondestructive manner.

Nakanishi et al. (2011, 2012) were the first to describe the use of fluorescence microscopy to study Mrp2 inhibition by drugs and/or drug metabolites in rat hepatocytes. These investigators looked at a change of fluorescence intensity in the bile canaliculi when potential Mrp2 inhibitors were added. In that way, it is difficult to differentiate between esterase inhibition on one hand and Mrp2 inhibition on the other: It is indeed possible that drugs and/or their metabolites affect the esterases converting CDFDA to CDF, which would also lead to a reduction of fluorescence intensity. In the present study, the fluorescence intensity was measured both in the cells and in the bile canaliculi, taking into account only the effect of drugs on Mrp2/MRP2. Indeed, potential inhibition of the intracellular esterase activity by the drug (metabolite) would not affect the BEI of CDF.

Another advantage of the present approach includes the possibility of specifically exploring the interference with Mrp2/MRP2-mediated transport at the canalicular membrane. For instance, it is well known that typical Mrp2/MRP2 inhibitors are quite often MRP3 inhibitors, and that CDF is not only a substrate for Mrp2/MRP2 but also for Mrp3/MRP3 (Zamek-Gliszczynski et al., 2003; Weiss et al., 2007). On the basis of unpublished in-house data, CDF is a good substrate for rat Mrp3, whereas it is a poor substrate for human MRP3. Since Mrp3/MRP3 is mainly present at the basolateral side of the hepatocyte membrane (König et al., 1999), it is probably involved in CDF efflux back into the medium (Zamek-Gliszczynski et al., 2003). However, very limited impact is expected from Mrp3/MRP3 (or other Mrp/MRP isoforms located at the basolateral membrane) on the BEI values of CDF in the present study.

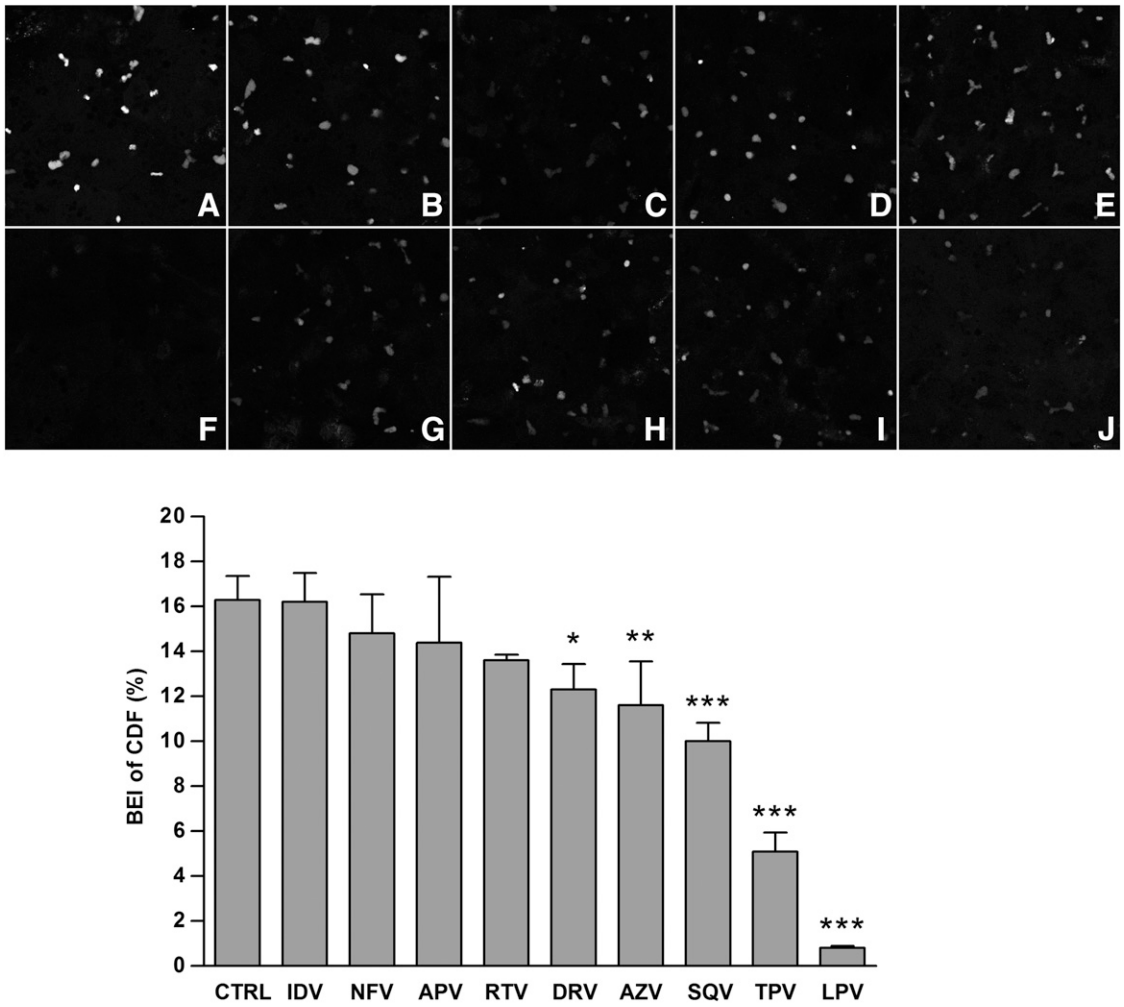

Fig. 3. Effect of HIV protease inhibitors on BEI of CDF in sandwich-cultured human hepatocytes at culture day 6. Cells were preincubated with HIV protease inhibitors (10 μM) for 10 minutes, prior to incubation with CDFDA (1 μM) for 10 minutes in absence or presence of HIV protease inhibitors. (A) Control, (B) amprenavir (APV), (C) atazanavir (AZV), (D) darunavir (DRV), (E) indinavir (IDV), (F) lopinavir (LPV), (G) nelfinavir (NFV), (H) ritonavir (RTV), (I) saquinavir (SQV), and (J) tipranavir (TPV). Bars represent the mean ± S.D. ($n = 3$). Statistical significance between the different conditions was evaluated using one-way analysis of variance followed by Dunnett's test. Significantly different from control condition; $^*P < 0.05$; $^{**}P < 0.01$; $^{***}P < 0.001$.

Additionally, it is known that CDFDA passively diffuses into the cells, whereas CDF relies on active uptake mediated by OATP. This means that compounds that can inhibit the reuptake of CDF could potentially lead to a decrease in the intracellular amounts of CDF, resulting in a decreased fluorescence intensity in our assay. As canalicular excretion is the driving force of CDF disposition (which can also be seen from the microscopic images), the impact of inhibition of CDF reuptake by OATP in the present assay would have been rather low. Moreover, the expression of uptake transporters, including the OATP family, decreases in SCRH/SCHH as a function of culture time (De Bruyn et al., 2013).

To correctly calculate the BEI on the basis of image analysis, saturation of pixel intensity had to be avoided. This was achieved by optimizing laser intensity, gain, and exposure time. An additional advantage of calculating the BEI on the basis of the image analysis is the shorter time required for data generation and processing (compared with using LC-based determination of cell/medium concentrations, for instance).

To our knowledge, this is an improved nondestructive assay that uses confocal imaging to calculate a BEI value and eventually to investigate Mrp2/MRP2 inhibition of drugs/metabolites in cultured hepatocytes using a fluorescent substrate. Most often, assays to screen for efflux transporter inhibitors in cultured cells rely on efflux studies that use both standard medium (bile canaliculi are intact) and Ca^{2+}/Mg^{2+}-free medium (bile canaliculi are disrupted) to calculate the accumulation of compounds in bile canaliculi, referred to as the conventional "offline" method (Ye et al., 2010). Also, transporter-expressed membrane vesicles and transporter-transfected cell lines are regularly used to screen for efflux transporter inhibitors (Förster et al., 2008; Lechner et al., 2010; Morgan et al., 2013). However, in that case, the formation of possible metabolites, which in their turn can lead to possible inhibitory effects, is ignored.

For the series of HIV protease inhibitors, a wide range in the extent of inhibition was observed in both SCRH and SCHH. In SCRH, a slight increase in the BEI of CDF in presence of amprenavir was noticed, for which the specific reason remains uncertain. As mentioned earlier, it would be improbable that this could be explained by interaction of amprenavir with Mrp3, which also has not to our knowledge been demonstrated in literature. There is a possibility that amprenavir increases the BEI of CDF by inhibiting Oatp in rat hepatocytes, which in fact was shown earlier (Annaert et al., 2010). Furthermore, it has been suggested that amprenavir is taken up by an unidentified transporter for

which CDF may be a substrate (Liu and Unadkat, 2013). However, it is also very improbable that amprenavir influences the efflux of CDF mediated by another known canalicular transporter, as it is shown that CDF is not a substrate for Bsep. However, in the same study, it was seen that CDF uptake by Bcrp-expressing membrane vesicles was approximately 29% of that by Mrp2, meaning that CDF is a weak substrate for Bcrp and thus can function as a partially selective substrate for Mrp2 (Nakanishi et al., 2012). Another study showed that amprenavir was not an inhibitor, nor a substrate for BCRP (Gupta et al., 2004). The CDF present in the medium may result from bile canaliculi intermittently releasing their contents or may be the result of sinusoidal efflux transport by the hepatocytes via Mrp3. Given the relatively short incubation time (10 minutes), the latter mechanism probably predominates in the current experimental conditions. A last hypothesis is that the increased BEI can be attributed to an activation of Mrp2 by amprenavir. However, no evidence was found on this mechanism.

Potent inhibitors for CDF efflux via Mrp2/MRP2 were lopinavir and tipranavir in both rat and human hepatocytes. Nelfinavir was also able to decrease the BEI in rat hepatocytes, but not in human, whereas darunavir, atazanavir and saquinavir were only able to inhibit CDF efflux in human hepatocytes. According to Ye et al. (2010), lopinavir, nelfinavir and indinavir were found to be the most potent Mrp2 inhibitors in rat hepatocytes, whereas in our study indinavir had no effect on the BEI of CDF in both rat and human hepatocytes, which is also the case for ritonavir. Our in vitro data are not entirely in accordance with what was found by others. For example, it has been shown previously that saquinavir and ritonavir are able to inhibit the Mrp2-mediated transport of methotrexate (Gutmann et al., 1999). However, this discrepancy is probably attributable to the different probe substrates used. This substrate dependency has been shown previously as it is known that MRP2 has more than one nonidentical binding site (Gerk et al., 2004) (Zelcer et al., 2003). Ye et al. (2010) have applied two Mrp2 substrates, namely CDF and estradiol-17-β-glucuronide, to investigate the possibility of Mrp2 inhibition by HIV protease inhibitors in the same in vitro model, which also resulted in substrate-dependent inhibitory effects. Therefore, a direct comparison between different studies using different probe substrates to investigate the effect of drug on Mpr2/MRP2-mediated transport is not always possible. Moreover, the difference in results between rat and human in the first place can be explained by a species difference in the amino acid sequence of the transporter. It was found that human MRP2 has 78% amino acid sequence identity with rat Mrp2 (Mazur et al., 2012). Moreover, a species difference in Mrp2/MRP2-mediated transport has been shown by several research teams. Additionally, the absolute amount of Mrp2 in rat is about 10-fold higher than the amount of MRP2 in human, as quantified by liquid chromatography–tandem mass spectrometry (Li et al., 2009).

A role for Mrp2/MRP2 in the hepatic disposition of HIV protease inhibitors has been reported in several in vitro studies. Saquinavir, ritonavir, and indinavir were identified as MRP2 substrates, and lopinavir was found to be a substrate for both at Mrp2 and human MRP2 (Huisman et al., 2002). However, Bierman et al. (2010) reported that several HIV protease inhibitors are poor substrates yet potent blockers for ABC transporters in general. In our study, especially lopinavir and saquinavir, but not indinavir, decreased the BEI of CDF to some extent in human hepatocytes.

As part of the present study, the current data were compared with data obtained from a study which was performed by our research team applying the conventional "offline" method (Ye et al., 2010). The Pearson correlation coefficient between these two data sets was relatively poor, especially for the data obtained with human hepatocytes. Nevertheless, the three least potent MRP2-inhibiting HIV protease inhibitors in the study of Ye et al. (amprenavir, indinavir, nelfinavir) also turn out to be least potent in the present study. Furthermore, the lack of pronounced MRP2-inhibiting properties of these three HIV protease inhibitors appears consistent with several other studies on the effects of these HIV protease inhibitors on MRP1 activity (Jones et al., 2001; van der Sandt et al., 2001; Bierman et al., 2010). At the other end of the spectrum, lopinavir, tipranavir, saquinavir, and atazanavir are the most potent MRP2-inhibiting HIV protease inhibitors in the present study. This "class of most potent" MRP2 inhibitors is largely in agreement with the data obtained by Ye et al., who reported at least 60% inhibition of MRP2 with the conventional method for lopinavir, saquinavir, and atazanavir. For the same HIV protease inhibitors (and including tipranavir), clear evidence was found in literature that they inhibit MRP1 and/or MRP2 (Agarwal et al., 2007; Janneh et al., 2008, 2009; Bierman et al., 2010). Taken together, there seems to be an acceptable agreement between the present and previously obtained data (including the data obtained by Ye et al.) with respect to MRP2 inhibitory potency toward HIV protease inhibitors. The relatively large variability (low precision) in the effect of several HIV protease inhibitors on the biliary excretion of CDF in the work by Ye et al. remains the most important major difference with the present study. In fact this may explain at least in part the lack of an excellent correlation between the data sets. This variability may be inherent in the conventional method, the basis of which is the assumption that bile canaliculi remain intact in the presence of media containing Ca^{2+} and Mg^{2+}. However, the present data also show that in the presence of standard buffer (containing Ca^{2+} and Mg^{2+}), bile canaliculi tend to open spontaneously and close (Supplemental Fig. 1). In a time interval of 70 minutes, some bile canaliculi had already opened within 5 minutes, whereas some remained closed throughout the entire experiment. The occurrence of bile canalicular contraction in sandwich culture has been described previously (Reif et al., 2015).

In view of extrapolating these findings on Mrp2/MRP2 inhibition to the in vivo situation, the question arises, To what extent does the hepatocyte/medium concentration ratio of the HIV protease inhibitor in vitro correspond to the liver/plasma concentration ratio of these drugs in vivo? Previously, we determined the Kp_{uu} (intracellular to extracellular unbound concentration ratio) values for ritonavir (Keemink et al., 2015) and atazanavir (Nicolaï et al., 2016) in rat and/or human hepatocytes. These investigations revealed that intracellular exposure to HIV protease inhibitor results from a complex interplay between extensive hepatic metabolism and uptake as well as efflux transport. As cytochrome P450-mediated metabolic capacity is significantly reduced in cultured primary hepatocytes, differences in intracellular exposure (owing to different accumulation kinetics and differences in metabolic clearances) compared with hepatocytes in vivo can be expected. It follows that future in vitro exploration of Mrp2/MRP2 inhibition should be conducted preferentially at extracellular concentrations, to yield intracellular hepatic exposure comparable to that observed during in vivo studies. PBPK models for HIV protease inhibitors that are currently in development (De Bruyn et al., 2016) should be instrumental in estimating these in vivo intrahepatic exposure values.

Conclusion

Confocal imaging allowed us to investigate the inhibitory effect of HIV protease inhibitors on the BEI of CDF in a very sensitive and nondestructive manner. The BEI calculated on the basis of confocal imaging supports a higher throughput and better precision compared with classic methods.

Acknowledgments

The authors thank the National Institutes of Health AIDS Research and Reference Reagent Program for providing the HIV protease inhibitors.

Authorship Contributions

Participated in research design: Holmstock, Snoeys, Annaert.

Conducted experiments: Holmstock.

Performed data analysis: Holmstock.

Wrote or contributed to the writing of the manuscript: Holmstock, Oorts, Snoeys, Annaert.

References

Agarwal S, Pal D, and Mitra AK (2007) Both P-gp and MRP2 mediate transport of Lopinavir, a protease inhibitor. *Int J Pharm* **339**:139–147.

Annaert P, Ye ZW, Stieger B, and Augustijns P (2010) Interaction of HIV protease inhibitors with OATP1B1, 1B3, and 2B1. *Xenobiotica* **40**:163–176.

Annaert PP, Turncliff RZ, Booth CL, Thakker DR, and Brouwer KLR (2001) P-glycoprotein-mediated in vitro biliary excretion in sandwich-cultured rat hepatocytes. *Drug Metab Dispos* **29**: 1277–1283.

Badée J, Achour B, Rostami-Hodjegan A, and Galetin A (2015) Meta-analysis of expression of hepatic organic anion-transporting polypeptide (OATP) transporters in cellular systems relative to human liver tissue. *Drug Metab Dispos* **43**:424–432.

Bierman WF, Scheffer GL, Schoonderwoerd A, Jansen G, van Agtmael MA, Danner SA, and Scheper RJ (2010) Protease inhibitors atazanavir, lopinavir and ritonavir are potent blockers, but poor substrates, of ABC transporters in a broad panel of ABC transporter-overexpressing cell lines. *J Antimicrob Chemother* **65**:1672–1680.

Bow DAJ, Perry JL, Miller DS, Pritchard JB, and Brouwer KLR (2008) Localization of P-gp (Abcb1) and Mrp2 (Abcc2) in freshly isolated rat hepatocytes. *Drug Metab Dispos* **36**: 198–202.

De Bruyn T, Chatterjee S, Fattah S, Keemink J, Nicolaï J, Augustijns P, and Annaert P (2013) Sandwich-cultured hepatocytes: utility for in vitro exploration of hepatobiliary drug disposition and drug-induced hepatotoxicity. *Expert Opin Drug Metab Toxicol* **9**:589–616.

De Bruyn T, Stieger B, Augustijns PF, and Annaert PP (2016) Clearance prediction of HIV protease inhibitors in man: role of hepatic uptake. *J Pharm Sci* **105**:854–863.

Ellis LCJ, Grant MH, Hawksworth GM, and Weaver RJ (2014) Quantification of biliary excretion and sinusoidal excretion of 5(6)-carboxy-2′,7′-dichlorofluorescein (CDF) in cultured hepatocytes isolated from Sprague Dawley, Wistar and Mrp2-deficient Wistar (TR(-)) rats. *Toxicol In Vitro* **28**:1165–1175.

Förster F, Volz A, and Fricker G (2008) Compound profiling for ABCC2 (MRP2) using a fluorescent microplate assay system. *Eur J Pharm Biopharm* **69**:396–403.

Gerk PM, Li W, and Vore M (2004) Estradiol 3-glucuronide is transported by the multidrug resistance-associated protein 2 but does not activate the allosteric site bound by estradiol 17-glucuronide. *Drug Metab Dispos* **32**:1139–1145.

Giacomini KM, Huang S-M, Tweedie DJ, Benet LZ, Brouwer KLR, Chu X, Dahlin A, Evers R, Fischer V, Hillgren KM, et al.; International Transporter Consortium (2010) Membrane transporters in drug development. *Nat Rev Drug Discov* **9**:215–236.

Gupta A, Zhang Y, Unadkat JD, and Mao Q (2004) HIV protease inhibitors are inhibitors but not substrates of the human breast cancer resistance protein (BCRP/ABCG2). *J Pharmacol Exp Ther* **310**:334–341.

Gutmann H, Fricker G, Drewe J, Toeroek M, and Miller DS (1999) Interactions of HIV protease inhibitors with ATP-dependent drug export proteins. *Mol Pharmacol* **56**:383–389.

Guyot C, Hofstetter L, and Stieger B (2014) Differential effects of membrane cholesterol content on the transport activity of multidrug resistance-associated protein 2 (ABCC2) and of the bile salt export pump (ABCB11). *Mol Pharmacol* **85**:909–920.

Heredi-Szabo K, Kis E, Molnar E, Gyorfi A, and Krajcsi P (2008) Characterization of 5(6)-carboxy-2,'7'-dichlorofluorescein transport by MRP2 and utilization of this substrate as a fluorescent surrogate for LTC4. *J Biomol Screen* **13**:295–301.

Huisman MT, Smit JW, Crommentuyn KML, Zelcer N, Wiltshire HR, Beijnen JH, and Schinkel AH (2002) Multidrug resistance protein 2 (MRP2) transports HIV protease inhibitors, and transport can be enhanced by other drugs. *AIDS* **16**:2295–2301.

Janneh O, Anwar T, Jungbauer C, Kopp S, Khoo SH, Back DJ, and Chiba P (2009) P-glycoprotein, multidrug resistance-associated proteins and human organic anion transporting polypeptide influence the intracellular accumulation of atazanavir. *Antivir Ther* **14**:965–974.

Janneh O, Hartkoorn RC, Jones E, Owen A, Ward SA, Davey R, Back DJ, and Khoo SH (2008) Cultured CD4T cells and primary human lymphocytes express hOATPs: intracellular accumulation of saquinavir and lopinavir. *Br J Pharmacol* **155**:875–883.

Jones K, Bray PG, Khoo SH, Davey RA, Meaden ER, Ward SA, and Back DJ (2001) P-Glycoprotein and transporter MRP1 reduce HIV protease inhibitor uptake in CD4 cells: potential for accelerated viral drug resistance? *AIDS* **15**:1353–1358.

Keemink J, Augustijns P, and Annaert P (2015) Unbound ritonavir concentrations in rat and human hepatocytes. *J Pharm Sci* **104**:2378–2387.

Köck K and Brouwer KLR (2012) A perspective on efflux transport proteins in the liver. *Clin Pharmacol Ther* **92**:599–612.

König J, Nies AT, Cui Y, Leier I, and Keppler D (1999) Conjugate export pumps of the multidrug resistance protein (MRP) family: localization, substrate specificity, and MRP2-mediated drug resistance. *Biochim Biophys Acta* **1461**:377–394.

Lechner C, Reichel V, Moenning U, Reichel A, and Fricker G (2010) Development of a fluorescence-based assay for drug interactions with human Multidrug Resistance Related Protein (MRP2; ABCC2) in MDCKII-MRP2 membrane vesicles. *Eur J Pharm Biopharm* **75**:284–290.

LeCluyse EL, Audus KL, and Hochman JH (1994) Formation of extensive canalicular networks by rat hepatocytes cultured in collagen-sandwich configuration. *Am J Physiol* **266**:C1764–C1774.

LeCluyse EL, Fix JA, Audus KL, and Hochman JH (2000) Regeneration and maintenance of bile canalicular networks in collagen-sandwiched hepatocytes. *Toxicol In Vitro* **14**:117–132.

Li N, Zhang Y, Hua F, and Lai Y (2009) Absolute difference of hepatobiliary transporter multidrug resistance-associated protein (MRP2/Mrp2) in liver tissues and isolated hepatocytes from rat, dog, monkey, and human. *Drug Metab Dispos* **37**:66–73.

Liu L and Unadkat JD (2013) Interaction between HIV protease inhibitors (PIs) and hepatic transporters in sandwich cultured human hepatocytes: implication for PI-based DDIs. *Biopharm Drug Dispos* **34**:155–164.

Lundquist P, Englund G, Skogastierna C, Lööf J, Johansson J, Hoogstraate J, Afzelius L, and Andersson TB (2014) Functional ATP-binding cassette drug efflux transporters in isolated human and rat hepatocytes significantly affect assessment of drug disposition. *Drug Metab Dispos* **42**:448–458.

Mazur CS, Marchitti SA, Dimova M, Kenneke JF, Lumen A, and Fisher J (2012) Human and rat ABC transporter efflux of bisphenol a and bisphenol a glucuronide: interspecies comparison and implications for pharmacokinetic assessment. *Toxicol Sci* **128**:317–325.

Morgan RE, van Staden CJ, Chen Y, Kalyanaraman N, Kalanzi J, Dunn RT, II, Afshari CA, and Hamadeh HK (2013) A multifactorial approach to hepatobiliary transporter assessment enables improved therapeutic compound development. *Toxicol Sci* **136**:216–241.

Nakanishi T, Ikenaga M, Fukuda H, Matsunaga N, and Tamai I (2012) Application of quantitative time-lapse imaging (QTLI) for evaluation of Mrp2-based drug-drug interaction induced by liver metabolites. *Toxicol Appl Pharmacol* **263**:244–250.

Nakanishi T, Shibue Y, Fukuyama Y, Yoshida K, Fukuda H, Shirasaka Y, and Tamai I (2011) Quantitative time-lapse imaging-based analysis of drug-drug interaction mediated by hepatobiliary transporter, multidrug resistance-associated protein 2, in sandwich-cultured rat hepatocytes. *Drug Metab Dispos* **39**:984–991.

Nicolaï J, De Bruyn T, Thevelin L, Augustijns P, and Annaert P (2016) Transport-metabolism interplay of atazanavir in rat hepatocytes. *Drug Metab Dispos* **44**:389–397.

Reif R, Karlsson J, Günther G, Beattie L, Wrangborg D, Hammad S, Begher-Tibbe B, Vartak A, Melega S, Kaye PM, et al. (2015) Bile canalicular dynamics in hepatocyte sandwich cultures. *Arch Toxicol* **89**:1861–1870.

van der Sandt IC, Vos CM, Nabulsi L, Blom-Roosemalen MC, Voorwinden HH, de Boer AG, and Breimer DD (2001) Assessment of active transport of HIV protease inhibitors in various cell lines and the in vitro blood–brain barrier. *AIDS* **15**:483–491.

Weiss J, Theile D, Ketabi-Kiyanvash N, Lindenmaier H, and Haefeli WE (2007) Inhibition of MRP1/ABCC1, MRP2/ABCC2, and MRP3/ABCC3 by nucleoside, nucleotide, and non-nucleoside reverse transcriptase inhibitors. *Drug Metab Dispos* **35**:340–344.

Wissel G, Kudryavtsev P, Ghemtio L, Tammela P, Wipf P, Yliperttula M, Finel M, Urtti A, Kidron H, and Xhaard H (2015) Exploring the structure-activity relationships of ABCC2 modulators using a screening approach. *Bioorg Med Chem* **23**:3513–3525.

Ye ZW, Camus S, Augustijns P, and Annaert P (2010) Interaction of eight HIV protease inhibitors with the canalicular efflux transporter ABCC2 (MRP2) in sandwich-cultured rat and human hepatocytes. *Biopharm Drug Dispos* **31**:178–188.

Zamek-Gliszczynski MJ, Xiong H, Patel NJ, Turncliff RZ, Pollack GM, and Brouwer KLR (2003) Pharmacokinetics of 5 (and 6)-carboxy-2′,7′-dichlorofluorescein and its diacetate promoiety in the liver. *J Pharmacol Exp Ther* **304**:801–809.

Zelcer N, Huisman MT, Reid G, Wielinga P, Breedveld P, Kuil A, Knipscheer P, Schellens JHM, Schinkel AH, and Borst P (2003) Evidence for two interacting ligand binding sites in human multidrug resistance protein 2 (ATP binding cassette C2). *J Biol Chem* **278**:23538–23544.

Address correspondence to: Dr. Pieter Annaert, Drug Delivery and Disposition, KU Leuven Department of Pharmaceutical and Pharmacological Sciences, Campus Gasthuisberg, O&N 2, Herestraat 49 box 921, B-3000 Leuven, Belgium. E-mail: Pieter.Annaert@kuleuven.be